19.3 An Overview of the May 10, 2003 Tornado Outbreak

Fred H. Glass

NOAA/National Weather Service
St. Charles, Missouri

1. INTRODUCTION

The period from May 4-10, 2003 was one of the most active severe weather periods documented in United States history. A record 393 tornadoes occurred across portions of the central and eastern U. S. (NOAA, 2003). The culminating event was an outbreak of 38 tornadoes across the middle and upper Mississippi Valley region on May 10th. Nine tornadoes were documented in northeast Missouri and west central Illinois (Fig. 1) within the county warning area (CWA) of the National Weather Service Office in St. Louis (LSX). Of the nine tornadoes, four of these were classified as strong (F2 or F3) and long-tracked with path lengths ≥ 10 miles. The Canton-Lima F2 tornado, which began in Lewis County, Missouri, had the longest documented track at 89 miles and a peak width of 300 yards. Despite damage estimated at 5-7 million dollars, there were no fatalities and only 10 minor injuries within the LSX CWA. This great fortune was due to the fact that the tornadoes occurred over primarily rural areas, and the tornado warnings had an average lead time of 23 minutes.

The large-scale pattern for this event could be coined *"synoptically evident"*. It featured a strong progressive mid-upper level trough and associated jet streak, and a deepening surface low with attendant boundaries moving through a very unstable air mass. Deep layer shear from the surface through 8 km of 38-47 m/s favored long-lived supercells (Bunkers et al. 2006 a, b).

Tornadoes defining this outbreak were produced by 9 discrete supercells. Late in the outbreak, several of the discrete supercells evolved into elongated hybrid supercell complexes containing several coexisting mesocyclones. All but 2 of the supercells produced families of tornadoes. The initial supercells developed in western Missouri and extreme southeast Kansas along and ahead of a pronounced pre-frontal trough/dryline. Other tornadic supercells formed across extreme north central Missouri and eastern Iowa in advance of the deepening surface low pressure system and attendant cold front.

The tornadoes across northeast Missouri and west central Illinois were produced by three discrete cyclic supercells. Each supercell produced multiple successively stronger tornadoes. While the large scale environment this day seemed supportive of tornadic supercells over a large portion of the central U.S., the majority of tornadoes were confined to the north of a retreating outflow boundary, where surface winds were backed and the lifting condensation level (LCL) heights were lower. Notable changes were observed in storm structure with each of the highlighted supercells after crossing the outflow boundary and prior to producing their strongest tornadoes. The three supercell thunderstorms morphed from classic "flying eagle" structures with low level appendages, to high precipitation structures with smaller

Corresponding author address: Fred H. Glass, NOAA/NWS, 12 Research Park Drive, St. Charles, MO 63304; email: fred.glass@noaa.gov

Fig 1. Map of tornado tracks (F-scale denoted) within the LSX CWA in northeast Missouri and west central Illinois.

overall dimensions. Storm splits and cells mergers were also noted, as well as an overall decrease in the highest radar reflectivity levels.

This study provides an overview of the important aspects of this event with focus on the three tornadic supercells which impacted the LSX CWA. A brief chronology of the supercells and their lifecycles in presented in section 2. Section 3 details the evolution and character of the outflow boundary, and its relationship to tornado production by the supercells. Important radar observations of the supercells' lifecycles are documented in section 4, along with concurrent observations of cloud-to-ground lightning activity. Particular attention is given to the time period when the supercells crossed the outflow boundary and when they commenced tornado production.

2. SUPERCELL DETAILS

Figure 2 is a plot of the tracks for 5 of the supercells. Initial cell positions and their time of development are noted at the first point, while the last point represents either a demise of the storm to below 35 dBZ or a merger with other cells. Table 1 summarizes important aspects of the supercells' lifecycles. Supercells A, B, and C initiated along and ahead of the pre-frontal trough/dryline between 1905 UTC *(hereafter all times UTC and year 2003)* and 2005, while supercell D initiated around 1945 near the triple point of the outflow boundary/cold front/prefrontal trough-dryline. The cells which evolved into supercells A, B, and D exhibited weak rotation within 20 minutes after their development, with supercell convective modes noted 40-50 minutes after initiation. Development of supercell C was somewhat slower. The storm cell proceeded through a series of mergers with other cells before becoming a supercell around 90 minutes after initiation. A strong cell which developed 5-10 km in the wake of supercell C became the longest-lived storm. This cell slowly intensified and acquired weak rotation as it tracked northeast in the wake of supercell C, acquiring supercell characteristics (supercell C') 45 minutes later. Supercell C'

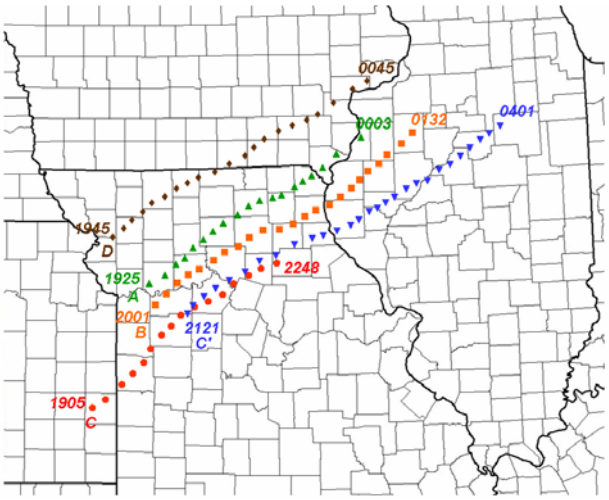

Fig 2. Plot of the maximum radar reflectivity centroid tracks of selected supercells (annotated A-D). The first point is the initial cell with subsequent positions every 15 minutes. Annotated times are UTC.

ID	Storm Life/ Supercell Life (h)	Initiation Time (UTC)	Time Supercell Status Achieved (UTC)	Bndry Crossing Time (UTC)	Time Of First Tornado (UTC)	# of Tornadoes
A	4.5/3.75	1925	2011	2045	2101	3
B	5.5/4.75	2001	2046	2205	2223	4
C	3.7/2.40	1905	2036			
C'	6.6/5.90	2121	2206	2310	2319	14
D	5.5/4.25	1945	2026		2137	2

Table 1. Important times and tornado count for the supercells.

then overtook and merged with supercell C. Tornado production for the supercells (A, B, C', D) did not commence until 0.8-1.6 hours (h) after supercell characteristics were first observed, and after the supercells completely crossed the outflow boundary. The original supercell C never produced a tornado before it was overtaken by C'. Additional discussion on the relationship of the outflow boundary to supercell tornado production will be given in section 3. Three of the supercells (B, C', D) qualified as long-lived following the criteria established by Bunkers et al. (2006a), while supercell A was moderate-lived (see Table 1). Supercell C' was the longest-lived at 5.9 h, and also produced the greatest number of tornadoes (14). It is interesting to note that when comparing supercells A-C', they were progressively longer-lived with southern extent. This may be a result of two factors: the speed and movement of the cold front and the breadth of the unstable air mass the supercells traversed.

3. MESOSCALE OUTFLOW BOUNDARY

Previous studies by Maddox (1980) and Markowski et al. (1998) have recognized the importance of preexisting mesoscale boundaries in tornado production. Boundaries act to organizing heat and moisture distributions and increase low-level horizontal vorticity, which enhances low-level mesocyclogenesis. The convective outflow boundary in this event was produced by a large mesoscale convective system (MCS). The MCS developed across western Missouri during the early morning hours of 10 May, and tracked eastward into

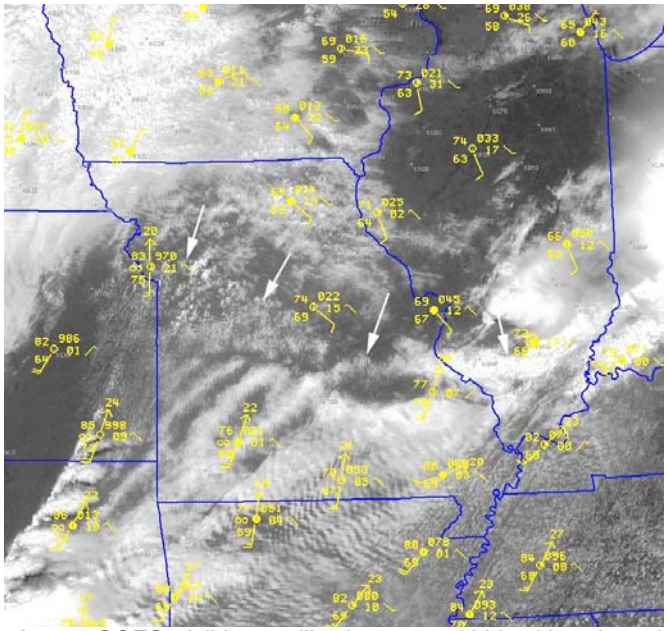

Fig 3. GOES visible satellite image at 1800 with selected METARS. Arrows denote position of the outflow boundary.

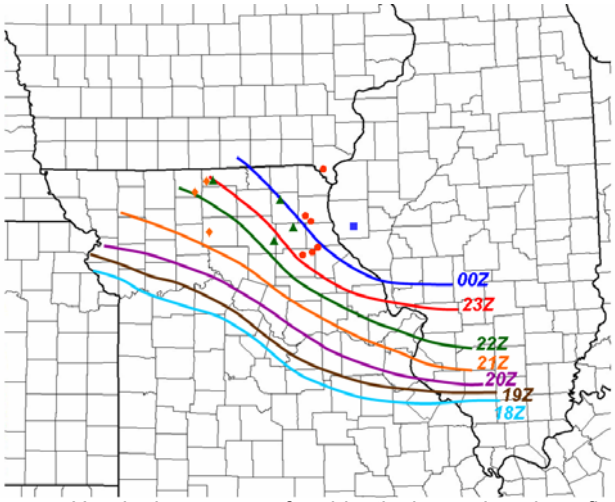

Fig 4. Hourly isocrones of subjectively analyzed outflow boundary positions from 1800 10 May until 0000 11 May. Annotated marks represent tornado touchdowns. Color of the marker corresponds to the hour proceeding the same colored boundary position (e.g. red markers are tornado touchdowns between 2300-2359.

the Ohio Valley by midday, leaving behind the well-defined outflow boundary in its wake. Figure 3 shows the position of the outflow boundary at 1800, extending from southern Illinois through central Missouri to just north of Kansas City, MO where it intersected the dryline. There was marked baroclinicity across boundary at this time and associated backing of the surface winds from southwesterly in the warm sector to southeasterly in the cool sector. Surface temperatures were in the upper 60s to lower 70s (°F) north of the boundary with dew points in the middle to upper 60s. South of the boundary, surface temperatures were the upper 70s to lower 80s with dew points in the lower 70s. The warm sector air mass south of the boundary was quite unstable and capped. A special 1800 Springfield (SGF) sounding located 165 km south-southwest of the boundary had a mean-layer

CAPE (MLCAPE) of 1989 J/kg with a lifted index (LI) of -6° C. An elevated mixed layer (EML) inversion was present resulting in a CIN of -35 J/kg, while the lifted condensation level (LCL) height was 668 m AGL and level of free convection (LFC) height was 2169 m AGL. The wind profile was unidirectional with southwesterly winds increasing with height, and 0-6 km bulk shear of 44 m/s and 0-8 km bulk shear of 47 m/s. Only slight veering was evident in the lowest 3 km resulting in 0-3 km storm relative helicity (SRH) values of 136 m^2/s^2. A 1800 00-h RUC sounding centered in northeast Missouri around 105 km north of the boundary was used to investigate properties of the cool sector air mass. A shallow moist low-level inversion was evident along with drying above the surface based layer, resulting in a low LCL/LFC height and a capped air mass with SBCAPE of less than 500 J/kg. The wind profile was dramatically different. The wind increased with height with pronounced veering in the lowest 2 km and southwesterly unidirectional flow aloft. The resultant hodograph showed significant low-level cyclonic curvature; 0-3 km SRH was 259 m^2/s^2.

Figure 4 shows positions of the outflow boundary between 1800 May 10 and 0000 May 11 annotated with tornado touchdown times. The position of the boundary was subjectively analyzed using visible satellite imagery, radar imagery, METAR observations, and supplemental surface observations from the University of Missouri Ag Weather stations. The boundary steadily lifted northeastward in advance of the migrating surface low and attendant pre-frontal trough/dryline during the afternoon and early evening hours. Baroclinicity gradually decreased as the boundary moved northward and relatively cloud-free skies in the cool sector allowed for ample heating. This heating combined with increasing low-level moisture and steepening mid-level lapse rates allowed the cool sector north of the boundary to destabilize. Storm Prediction Center (SPC) mesoanalysis graphics from 2200 indicated the region across northeast Missouri along and north of the outflow boundary was quite favorable for tornadic supercells. MLCAPE had increased to 2000-2500 J/kg, while the low surface dew point depressions (*often used as a proxy for LCL height*) resulted in LCL and LFC heights below 800 m AGL. The backed southeasterly surface winds combined with a strengthening LLJ resulted in 0-1 km SRH values greater than 250 m^2/s^2 (Fig 5).

Storms A-C' were supercells for anywhere from 0.5-1.4 h before crossing the outflow boundary. All of them then proceeded to produce their first tornado within 20 minutes of crossing the outflow boundary (see Table 1), and no greater than 20 km into the cool sector. The time matched plot of the hourly tornado touchdowns relative to the boundary position in Figure 4 shows all of the tornadoes from the supercells occurred on the cool side of the outflow boundary.

4. STORM CHARACTERISTICS AND EVOLUTION

High resolution (8 bit) radar data from the WSR-88Ds at Pleasant Hill, MO (KEAX), St. Louis, MO (KSTL), and Lincoln, IL (KILX), as well as lower resolution (4 bit) WSR-88D radar data from Des Moines, IA (KDMX), Davenport, IA (KDVN), and Springfield, MO (KSGF) were used in this study. Time series plots of selected radar parameters [cell-based vertically integrated liquid (VIL), maximum reflectivity (dBZ) height, echo top (ET) height, lowest-elevation rotational velocity (Vr) magnitude] were constructed using data from the nearest WSR-88D radar to illustrate changes in storm intensity. It should be noted that the supercells were viewed

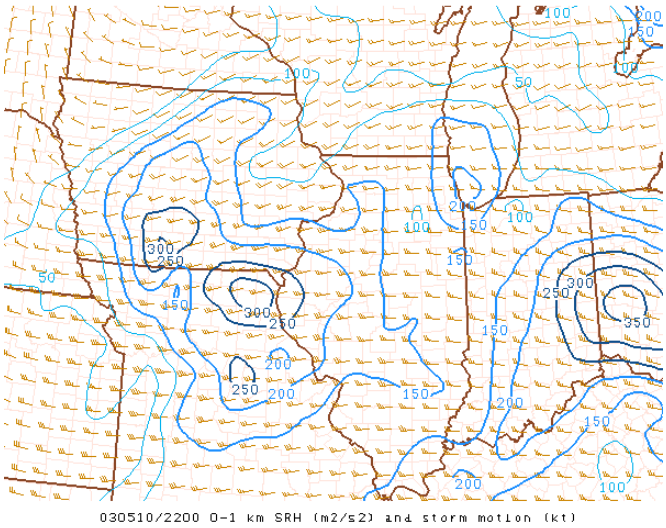

Fig 5. SPC mesoanalysis graphic of 0-1 km SRH m^2/s^2) valid 2200 10 May.

at long ranges (≥130 km) from all of the radars for the majority of the period when they produced severe weather. Due to radar sampling issues at long ranges, this can lead to fluctuations in the cell-based radar parameters (Johnson et al. 1998; Stumpf et al. 2004). Storm motion at a significant angle to the radar, and broadening of the radar beam diameter at these ranges can also result in failure to measure peak radial velocities associated with mesocyclones. This was occasionally observed with all of the storms. Cloud-to-ground (CG) lightning data was extracted from 5 minute plots available on the NWS Advanced Weather Information Processing System (AWIPS).

a. Supercell A

Supercell A developed at 1925 along the pre-frontal trough/dryline in Ray County in west-central Missouri (Fig. 2). The storm grew and exhibited weak rotation by 1945, becoming a supercell with a weak mesocyclone at 2011. Upon crossing the outflow boundary at 2045, the storm rapidly intensified with a new mesocyclone developing on the southeast flank. The supercell produced a brief F0 tornado at 2101. The time series in Figure 6a shows the supercell reached peaked intensity at the time of the tornado with a VIL of 64 kg/m^2 and max reflectivity at a height of 25.0 kft AGL. The rotational velocity associated with the strengthening mesocyclone maximized at 48 kts just prior to the tornado. Coinciding with the supercell crossing the boundary and intensifying, there was a large increase in the total CG flash rate (Fig. 6b) After peaking, the flash rate then decreased just as quickly by the time of the tornado, with positive CG lightning briefly dominating the total flash count after the tornado.

The supercell became quite strong as it moved northeast through the cool sector displaying a classic structure and periodic three body scatter spike (TBSS) signatures. Left moving cell splits were frequently observed, but these cells moved quickly northeast and dissipated. Overall the storm maintained a quasi-steady state through 2151 with only minor fluctuations in the overall intensity, likely due to pulsating updrafts. After 2151 the supercell dramatically weakened with a corresponding decrease in CG

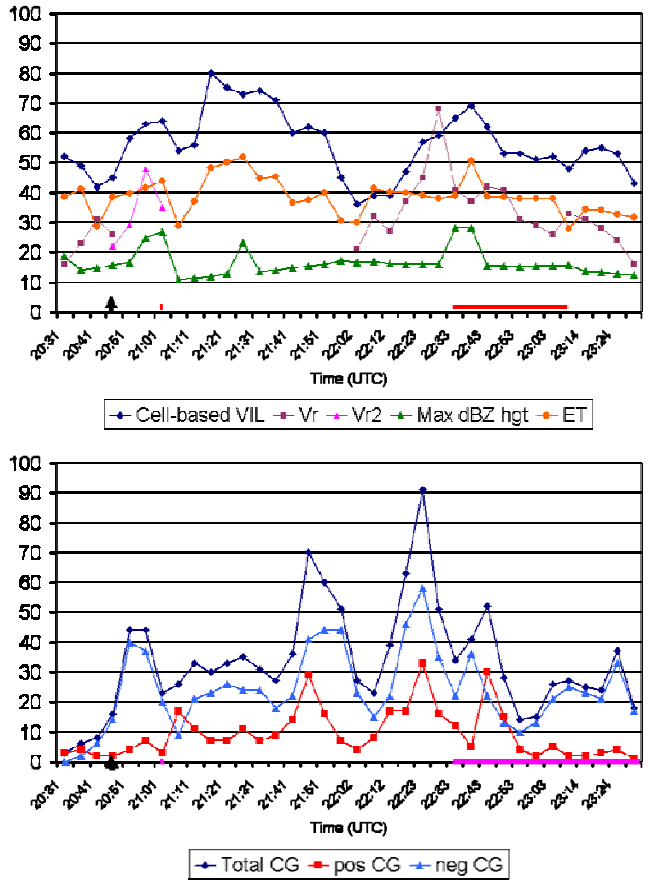

Fig 6. Time series plots for supercell A of: (a) cell-based VIL (kg/m^2), ET (kft AGL), maximum reflectivity height (kft AGL), and 0.5° Vr (kts), and (b) 5-min total CG lightning, 5-min positive CG lightning, and 5-min negative CG lightning. Boundary crossing time (arrow) and tornado times (thick line) annotated along the time axis.

lighting. Between 2218 and 2238 the supercell then cycled back upward with the development of a new intense updraft and strong mesocyclone on the southeast flank, and a left-moving cell split on the northern flank. Figure 7 shows the resulting tornadic supercell had diminished in size and intensity from one hour earlier. An F2 tornado touched down in Knox County at 2333 shortly after the mesocyclone exhibited a maximum Vr of 68 kts, and as the VIL, max reflectivity height, and ET peaked (Fig. 6a). The CG flash rate displayed similar trends as the first tornado occurrence. There was a significant increase to 91 flashes/5-min as the supercell was intensifying, followed by a marked decrease by the time of the tornado. These lightning trends are likely a reflection of the changes in the updraft/downdraft structure of the supercell, with the increase marking the updraft intensification phase and the decrease due to an intensifying rear flank downdraft (RFD) prior to tornadogenesis.

b. Supercell B

Supercell B developed at 2001 in advance of the pre-frontal trough/dryline and in the wake of another thunderstorm across Lafayette County (Fig. 2). Similar to supercell A, it exhibited weak rotation relatively soon. The rotation strengthened and deepened enough for the storm to be

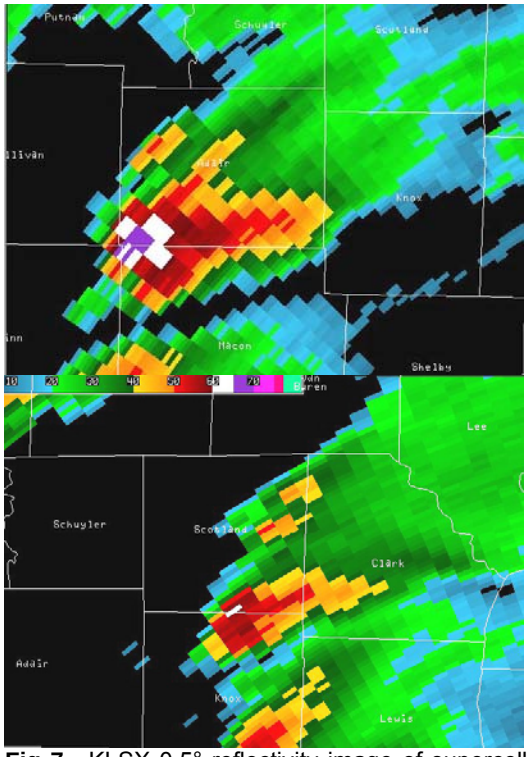

Fig 7. KLSX 0.5° reflectivity image of supercell A at (a-top) 2137 UTC and (b-bottom) 2238 UTC.

deemed a supercell by 2046. The supercell went through a series of cell mergers over the following 1.5 h, initially strengthening then achieving a quasi-steady state. VIL values as high as 83 kg/m^2 were observed at 2131 (Fig. 8a). CG lightning activity which had been nearly non-existent early in its life, increased steadily after 2115 peaking at 120 flashes/5-min just prior to crossing the outflow boundary (Fig. 8b). Just prior to crossing the outflow boundary at 2205, the storm began a strengthening trend including the development of a new mesocyclone on the southeast flank. The strengthening accelerated after the supercell crossed the outflow boundary and underwent a left-moving cell split. VIL values as high as 84 kg/m^2 and a TBSS were observed when the first tornado touched down in eastern Macon County at 2223 (Fig. 8a). Rotational velocities show the mesocyclone strengthened to moderate-strong intensity (Vr=33-41kts at 105 nm) prior to and after the tornado touchdown. This first tornado was on the ground until 2234 followed by a second touchdown at 2243. A deep high reflectivity core, moderate-strong mesocyclone, and TBSS were observed continuously during this period. Dramatic changes occurred with supercell B after 2253. After displaying classic structure for several hours, the supercell underwent a striking transformation, diminishing in overall size and intensity during the time of its strongest tornado (Fig. 9). This transition occurred as the original mesocyclone occluded, a new strong mesocyclone developed on the southeast flank, and a series of left-moving cell splits were observed. Figure 8a shows that VIL values decreased from 77 kg/m^2 at 2258 prior to the F2 tornado, to 31 kg/m^2 at 2354 when the long-track tornado had been on the ground for 46 minutes. The fluctuations seen in the Vr2 trace with the new mesocyclone appear to be a result of radar sampling issues.

The CG lightning trends for supercell B show some similarities and differences when compared to supercell A. A

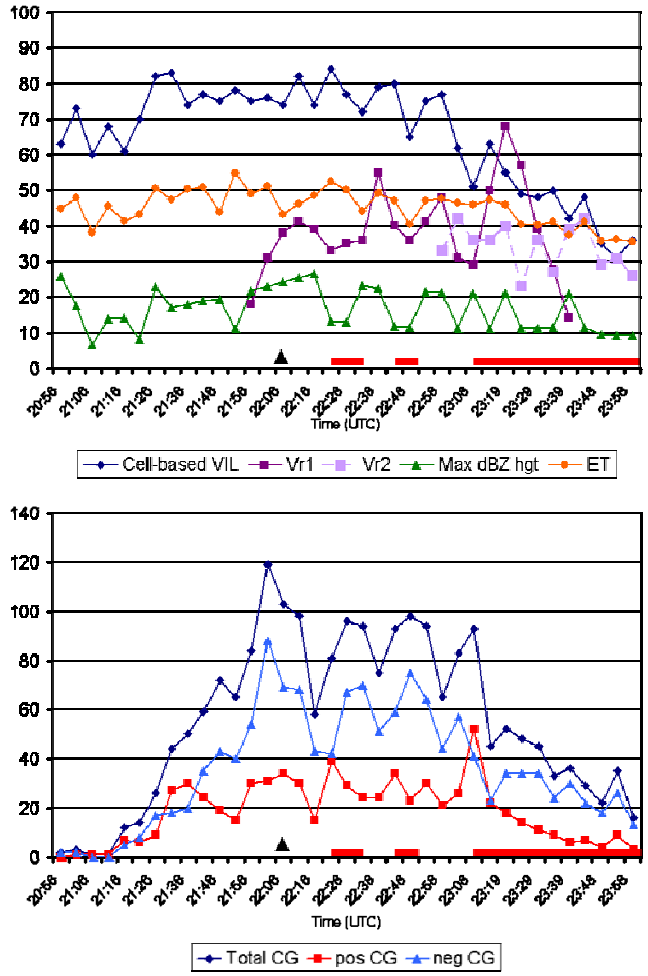

Fig 8. Same as Figure 6 except for supercell B.

decrease in CG activity followed by an increase is noted before the first two F0 tornadoes (Fig. 8b). Prior to the F2 tornado, a decrease in CG flash count is evident with the development of the new mesocyclone, which is then followed by an increase. The CG flash count then is observed to decrease substantially by the time of the F2 tornado and continue decreasing thereafter.

c. Supercell C'

Supercell C' was the most prolific tornado producer of the event, was the southern-most tornadic supercell, and displayed perhaps the most complex evolution. Supercell C' evolved from cells which developed 5-10 km in the wake of supercell C. Supercell C developed at 1905 in Bourbon County, KS along the pre-frontal trough/dryline (Fig. 2). Initially it struggled to intensify, but after a continuous series of mergers with other cells, it became a supercell around 2036. By 2121 new cells began developing along the flanking line of supercell C. These cells intensified, and by 2206 a new supercell with a weak mesocyclone was born. Through 2231 the 2 supercells strengthened as they tracked northeast in tandem with their main updrafts separated by as much as 15 km. The storm motion of the rear supercell C' was around 2.2 m/s faster, and between 2236 and 2253 the storms merged as supercell C' overtook supercell C.

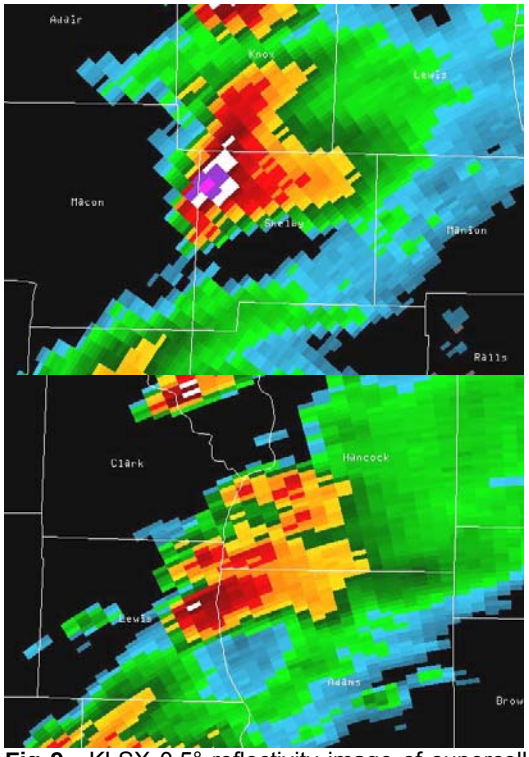

Fig 9. KLSX 0.5° reflectivity image of supercell B at (a-top) 2228 UTC and (b-bottom) 2329 UTC.

Supercell C' strengthened and developed a new mesocyclone after the merger, then crossed the outflow boundary a short time later at 2310. The storm continued to strengthen after crossing the boundary, exhibiting a moderate-strong mesocyclone, TBSS, and VIL of 78-80 kg/m^2 when it produced its first brief tornado at 2319 (Fig. 10a). Following this tornado, a new deep and intense mesocyclone developed on the southeast flank. This mesocyclone exhibited Vr values of 58 kts (Vr2 in Fig. 10a) as the supercell produced a second longer-track tornado near Monroe City. Similar to supercells A and B, supercell C' then began a structural transformation while producing a F3 tornado near Ely. The overall size and intensity of the storm diminished after a series of left-moving cell splits, and new cell mergers on the southwest flank (Fig. 11). While continuing to exhibit cyclic behavior, the overall intensity and size of the supercell continued to diminish after the F3 Ely tornado with VIL values decreasing to 42 kg/m^2 near the start of its 4th tornado at 0020 May 11 (Fig. 10a). The storm re-intensified again during this tornado, but exhibited an elongated quasi-linear structure. The supercell continued to evolve as it moved northeast into west-central Illinois, containing several co-existing parent mesocyclones and producing 10 additional tornadoes.

The CG lightning activity for supercell C' is shown in Figure 10b. There was a large increase in the flash rate following the merger with supercell C, which peaked after the storm crossed the outflow boundary. A steady overall decrease was evident through the time of the first 2 tornadoes and into the beginning of the third and strongest tornado. This was followed by a brief increase in flash activity between 2345 and 2355 while the third tornado was on the ground. A continuous decrease in the overall CG flash rate was then observed prior to and after the beginning of the 4th tornado. This later decrease in the flash rate coincided with

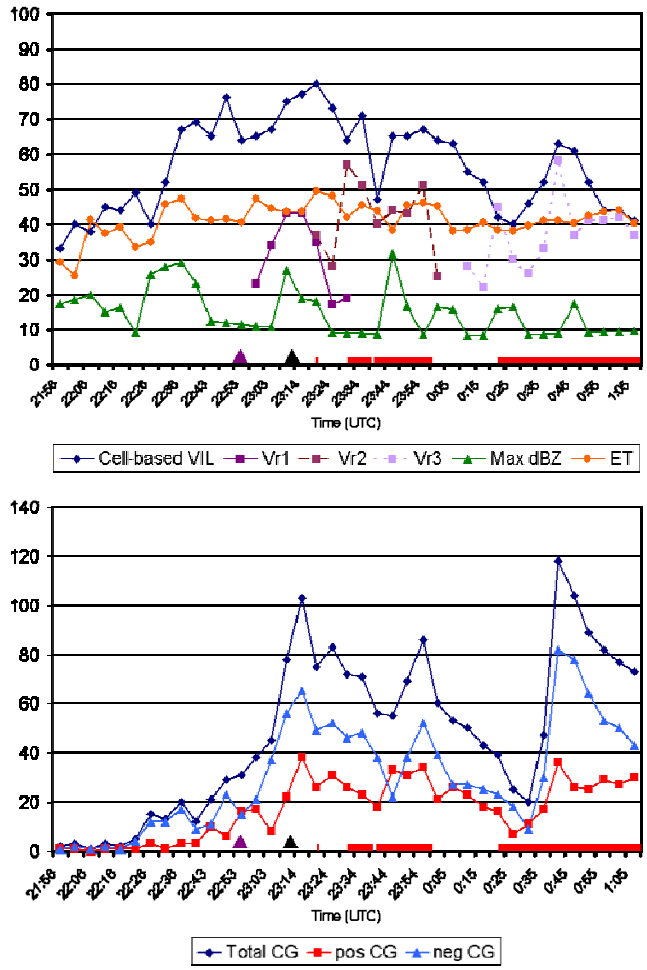

Fig 10. Same as Figure 6 except for supercell C'. *(first arrow denotes merger time)*.

the overall shrinking of the storm, and was followed by an equally dramatic increase between 0030 and 0040 associated with the storm intensification during the 4th tornado.

5. CONCLUDING REMARKS/SUMMARY

An outbreak of 38 tornadoes occurred across the central U.S. on 10-11 May 2003. The tornadoes were produced by 9 supercells or supercell clusters. The majority of the tornadoes across northeast Missouri and west central Illinois were produced by 3 discrete cyclic supercells. These later storms developed along and ahead of a prefrontal trough/dryline and attendant deepening surface low, in an environment favorable for supercell thunderstorms. Tornado production with the supercells however did not occur until well into their lifecycle, and commenced when the supercells crossed an "old" retreating outflow boundary leftover from an earlier MCS. North of the boundary the surface wind was backed resulting in strong low-level shear, and LCL heights were suppressed due to low surface temperature-dew point spreads. The storm structure changed after the three supercells crossed the boundary and prior to each producing its strongest tornadoes. The supercells morphed from classic "flying eagle" structures with high reflectivity levels and appendages, to quasi-high precipitation structures with

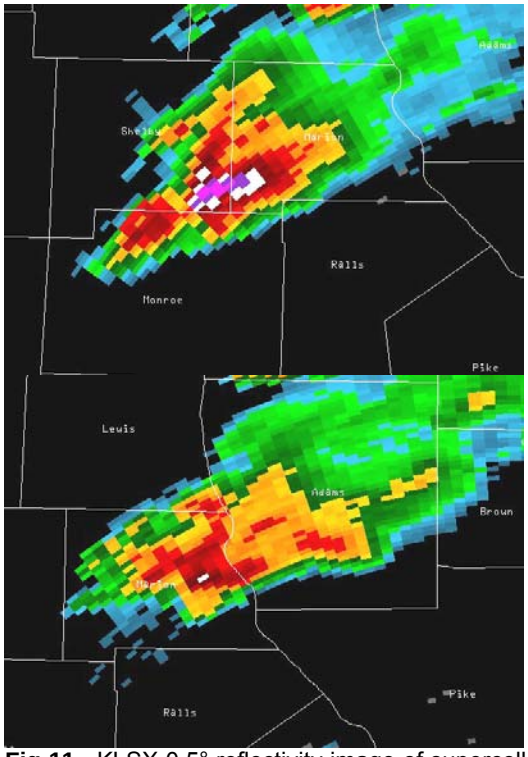

Fig 11. KLSX 0.5° reflectivity image of supercell C' at (a-top) 2324 UTC and (b-bottom) 2354 UTC.

smaller horizontal and vertical dimensions and lower peak radar reflectivity levels. Gilmore and Wicker (2002) also found this type of storm behavior and tornado production with supercells which crossed an outflow boundary on 2 June 1995. Storm scale features such as cell mergers and splits were observed with all 3 supercells, which frequently lead to an overall change in supercell intensity and/or structure. Observations of CG lightning flash rates show the storms were dominated by negative CG flash rates similar to findings by Carey et al. (2003). No coherent trends in polarity reversal were exhibited by the storms, however there was a general tendency for decreasing overall CG flash rates prior to a majority of the tornadoes.

6. ACKNOWLEDGEMENTS

Thanks to Mark Britt for his assistance using Excel and formatting some of the diagrams, and to Doug Tilly for his assistance with the sounding data. Finally thanks are extended to Steven Thomas (MIC) and Ron Przybylinksi (SOO) for administrative and scientific support.

7. REFERENCES

See http://www.crh.noaa.gov/lsx/?=science